

Axisymmetric Swirling Motion of Viscoelastic Fluid Flow Inside a Slender Surface of Revolution

Fernando Carapau *

Abstract—Motivated by the aim of modelling the behavior of swirling flow motion, we present a 1D hierarchical model for an Rivlin-Ericksen fluid with complexity $n = 2$, flowing in a circular straight tube with constant and no constant radius. Integrating the equation of conservation of linear momentum over the tube cross-section, with the velocity field approximated by the Cosserat theory, we obtain a one-dimensional system depending only on time and on a single spatial variable. The velocity field approximation satisfies both the incompressibility condition and the kinematic boundary condition exactly. From this new system, we derive the equation for the wall shear stress and the relationship between average pressure gradient, volume flow rate and swirling scalar function over a finite section of the tube. Also, we obtain the corresponding partial differential equation for the swirling scalar function.

Keywords: 1D model, wall shear stress, average pressure gradient, volume flow rate, swirling flow motion, viscoelastic fluids.

1 Introduction

In recent years the Cosserat theory approach has been applied in the field of fluid dynamics (see *e.g.* [1], [2], [3], [4], [16]) to reduce the full 3D system of equations of the flow motion into a system of partial differential equations which, apart from the dependence on time, depends only on a single spatial variable. The basis of this theory (see Duhem [9], Cosserat [7]) is to consider an additional structure of deformable vectors (called directors) assigned to each point on a space curve (the Cosserat curve). The relevance of using a director theory related to fluid dynamics is not in regarding the equations as approximations to three-dimensional equations, but rather in their use as independent theories to predict some of the main properties of three-dimensional problems, see *e.g.* [13],

[14]. Several important features of a director theory are: (i) the director theory incorporates all vector components of the equation of linear momentum; (ii) it is a hierarchical theory, making it possible to increase the accuracy of the model; (iii) the system of equations is closed at each order and therefore unnecessary to make assumptions about form of the nonlinear and viscous terms; (iv) invariance under a superposed rigid body motion is satisfied at each order; (v) the wall shear stress enters directly as a dependent variable in the formulation; (vi) the director theory has been shown to be useful for modeling flow in curved tubes, considering many more directors than in the case of a straight tube. A detailed discussion about the Cosserat theory can be found in [13], [14]. In this work, we use this theory to predict some of the main properties of a three-dimensional given problem where the fluid velocity field $\boldsymbol{\vartheta}(x_1, x_2, z, t) = \vartheta_i(x_1, x_2, z, t)\mathbf{e}_i$ can be approximated by (see Caulk and Naghdi [6])

$$\boldsymbol{\vartheta} = \mathbf{v} + \sum_{N=1}^k x_{\alpha_1} \dots x_{\alpha_N} \mathbf{W}_{\alpha_1 \dots \alpha_N}, \quad (1)$$

with¹

$$\mathbf{v} = v_i(z, t)\mathbf{e}_i, \quad \mathbf{W}_{\alpha_1 \dots \alpha_N} = W_{\alpha_1 \dots \alpha_N}^i(z, t)\mathbf{e}_i. \quad (2)$$

Here, \mathbf{v} represents the velocity along the axis of symmetry z at time t and $x_{\alpha_1} \dots x_{\alpha_N}$ are the polynomial base functions with order k (this number identifies the order of hierarchical theory and is related to the number of directors). Moreover, the vectors $\mathbf{W}_{\alpha_1 \dots \alpha_N}$ are the director velocities which are symmetric with respect to their indices and \mathbf{e}_i are the associated unit basis vectors. In this work, we apply the nine-director theory (this means $k = 3$ in equation (1)) to study a specific viscoelastic fluid model with swirling motion. We use nine directors because this is the minimum number for which the incompressibility condition and the kinematic boundary conditions on the lateral surface of the tube are satisfied pointwise. Using this theory, we obtain the unsteady relationship between

*This work has been partially supported by the research center CIMA/UE, FCT Portuguese funding program. The author Fernando Carapau is a Auxiliar Professor at the Departamento de Matemática and Centro de Investigação em Matemática e Aplicações (CIMA) da Universidade de Évora, Rua Romão Ramalho, N°59, 7000-651, Évora-Portugal (e-mail: flc@uevora.pt).

¹Latin indices subscript take the values 1, 2, 3; greek indices subscript 1, 2, and the usual summation convention is employed over a repeated index.

average pressure gradient and volume flow rate over a finite section of a straight circular tube with constant and no constant radius. Also, we obtain the corresponding equation for the wall shear stress and the partial differential equation for the swirling scalar function. Here in this work we extend the results obtain on [5].

2 System Description

Let x_i ($i = 1, 2, 3$) be the rectangular cartesian coordinates and for convenience set $x_3 = z$. We consider a homogeneous fluid moving within a circular straight and impermeable tube, the domain Ω (see Fig.1) contained in \mathbb{R}^3 . At the domain Ω , the boundary $\partial\Omega$ is composed by:

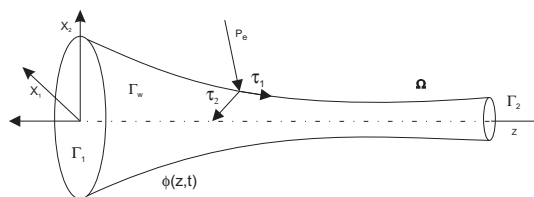


Figure 1: General fluid domain Ω with the tangential components of the surface traction vector τ_1 , τ_2 and p_e , where $\phi(z, t)$ denote the radius of the domain surface along the axis of symmetry z at time t .

the proximal cross-section Γ_1 , the distal cross-section Γ_2 and the lateral wall of the tube, denoted by Γ_w . Also, let us consider the surface scalar function $\phi(z, t)$, this function is related with the cross-section of the tube by the following relationship

$$\phi^2(z, t) = x_1^2 + x_2^2. \quad (3)$$

The three-dimensional equations governing the motion of an incompressible Rivlin-Ericksen fluid with complexity $n = 2$, without body forces, defined in a straight circular tube Ω with lateral wall Γ_w , is given by (in $\Omega \times (0, T)$)

$$\begin{cases} \rho \left(\frac{\partial \vartheta}{\partial t} + \vartheta \cdot \nabla \vartheta \right) = \nabla \cdot \mathbf{T}, \\ \nabla \cdot \vartheta = 0, \\ \mathbf{T} = -p\mathbf{I} + \mu \mathbf{A}_1 + \alpha_1 \mathbf{A}_2 + \alpha_2 \mathbf{A}_1^2, \quad \mathbf{T}_w = \mathbf{T} \cdot \varpi, \end{cases} \quad (4)$$

with the initial condition

$$\vartheta(x, 0) = \vartheta_0(x) \text{ in } \Omega, \quad (5)$$

and the homogeneous Dirichlet boundary condition

$$\vartheta(x, t) = 0 \text{ on } \Gamma_w \times (0, T), \quad (6)$$

where p is the pressure, $-p\mathbf{I}$ is the spherical part of the stress due to the constraint of incompressibility and ρ is

the constant fluid density. Equation (4)₁ represents the balance of linear momentum and (4)₂ is the incompressibility condition. In equation (4)₃, \mathbf{T} is the constitutive equation, \mathbf{T}_w denotes the stress vector on the surface Γ_w whose outward unit normal vector is ϖ . Also, μ is the constant fluid viscosity, α_1 and α_2 are viscoelastic coefficients usually called the normal stress moduli and the kinematic first two Rivlin-Ericksen tensors \mathbf{A}_1 and \mathbf{A}_2 are given by (see Rivlin and Ericksen [15])

$$\mathbf{A}_1 = \nabla \vartheta + (\nabla \vartheta)^T \quad (7)$$

and

$$\mathbf{A}_2 = \frac{\partial}{\partial t}(\mathbf{A}_1) + \vartheta \cdot \nabla \mathbf{A}_1 + \mathbf{A}_1 \nabla \vartheta + (\nabla \vartheta)^T \mathbf{A}_1. \quad (8)$$

The components of the outward unit normal vector ϖ to the surface $\phi(z, t)$ are²

$$\varpi_1 = \frac{x_1}{\phi \sqrt{1 + \phi_z^2}}, \quad \varpi_2 = \frac{x_2}{\phi \sqrt{1 + \phi_z^2}}, \quad \varpi_3 = -\frac{\phi_z}{\sqrt{1 + \phi_z^2}}. \quad (9)$$

The classical constitutive equation related with Newtonian fluids is recovered with $\alpha_1 = \alpha_2 = 0$ at condition (4)₃.

The thermodynamics and stability of the fluids related with the constitutive equation (4)₃ have been studied in detail by Dunn and Fosdick (see [10]), who showed that if the fluid is to be compatible with thermodynamics in the sense that all motions of the fluid meet the Clausius-Duhem inequality and the assumption that the specific Helmholtz free energy of the fluid is a minimum in equilibrium, then

$$\mu \geq 0, \quad \alpha_1 \geq 0, \quad \alpha_1 + \alpha_2 = 0. \quad (10)$$

Later, Fosdick and Rajagopal (see [11]) based on the experimental observation, showed that for many non-Newtonian fluids of current rheological interest the reported values for α_1 and α_2 do not satisfy the restriction (10)_{2,3}, relaxed that assumption. Also, they showed that for arbitrary values of $\alpha_1 + \alpha_2$, with $\alpha_1 < 0$, a fluid filling a compact domain and adhering to the boundary of the domain exhibits an anomalous behavior not expected on real fluids. The condition (10)₃ simplifies substantially the mathematical model and the corresponding analysis. The fluids characterized by (10) are known as second-grade fluids as opposed to the general second-order fluids (see *e.g.* [11]). It should also be added that the use of Clausius-Duheim inequality is the subject matter of much controversy (see *e.g.* Coscia and Galdi [8]). In the sequel we consider the system (3) – (8) with $\mu \geq 0$, $\alpha_1 < 0$ and $\alpha_1 + \alpha_2$ is an arbitrary value.

²Here a subscripted variable denotes partial differentiation.

Now, using the director theory approach (1) it follows from Caulk and Naghdi (see [6]) that the approximation of the velocity field $\boldsymbol{\vartheta} = \vartheta_i(x_1, x_2, z, t)\mathbf{e}_i$, with nine directors, is given by

$$\begin{aligned} \boldsymbol{\vartheta} &= \left[x_1(\xi + \sigma(x_1^2 + x_2^2)) - x_2(\omega + \eta(x_1^2 + x_2^2)) \right] \mathbf{e}_1 \\ &+ \left[x_1(\omega + \eta(x_1^2 + x_2^2)) + x_2(\xi + \sigma(x_1^2 + x_2^2)) \right] \mathbf{e}_2 \\ &+ \left[v_3 + \gamma(x_1^2 + x_2^2) \right] \mathbf{e}_3, \end{aligned} \quad (11)$$

where $\xi, \omega, \gamma, \sigma, \eta$ are scalar functions of the spatial variable z and time t . The scalar functions in (11) have the following physical meaning: γ is related to transverse shearing motion, ω and η are related to rotational motion (also called swirling motion) about \mathbf{e}_3 , while ξ and σ are related to transverse elongation. Also, from the work of Caulk and Naghdi (see [6]), the stress vector \mathbf{T}_w (see (4)₃) on the lateral surface Γ_w in terms of the outward unit normal vector $\boldsymbol{\varpi}$ and tangential components τ_1, τ_2, p_e is given by

$$\mathbf{T}_w = \tau_1 \boldsymbol{\lambda} - p_e \boldsymbol{\varpi} + \tau_2 \mathbf{e}_\theta, \quad (12)$$

where $\boldsymbol{\lambda}, \mathbf{e}_\theta$ are unit tangent vectors defined by

$$\mathbf{e}_\theta = \frac{x_\alpha}{\phi} \mathbf{e}_{\alpha\beta} \mathbf{e}_\beta, \quad \boldsymbol{\lambda} = \boldsymbol{\varpi} \times \mathbf{e}_\theta, \quad (13)$$

so that $(\boldsymbol{\lambda}, \boldsymbol{\varpi}, \mathbf{e}_\theta)$ form a right-handed triad, with $\mathbf{e}_{\alpha\beta}$ the permutation symbol defined by

$$\mathbf{e}_{11} = \mathbf{e}_{22} = 0, \quad \mathbf{e}_{12} = -\mathbf{e}_{21} = 1.$$

Using equations (9) and (13), the expression for the stress vector (see (4)₃) can be rewritten as

$$\begin{aligned} \mathbf{T}_w &= \left[\frac{1}{\phi(1 + \phi_z^2)^{1/2}} (\tau_1 x_1 \phi_z - p_e x_1 - \tau_2 x_2 (1 + \phi_z^2)^{1/2}) \right] \mathbf{e}_1 \\ &+ \left[\frac{1}{\phi(1 + \phi_z^2)^{1/2}} (\tau_1 x_2 \phi_z - p_e x_2 + \tau_2 x_1 (1 + \phi_z^2)^{1/2}) \right] \mathbf{e}_2 \\ &+ \left[\frac{1}{(1 + \phi_z^2)^{1/2}} (\tau_1 + p_e \phi_z) \right] \mathbf{e}_3, \end{aligned} \quad (14)$$

where the tangential component τ_1 is the wall shear stress.

Averaged quantities such as flow rate and average pressure are needed to study 1D models. Consider $S(z, t)$ as a generic axial section of the tube at time t defined by the spatial variable z and bounded by the circle defined in (3) and let $A(z, t)$ be the area of this section $S(z, t)$. Then, the volume flow rate Q is defined by

$$Q(z, t) = \int_{S(z, t)} \vartheta_3(x_1, x_2, z, t) da, \quad (15)$$

and the average pressure \bar{p} , by

$$\bar{p}(z, t) = \frac{1}{A(z, t)} \int_{S(z, t)} p(x_1, x_2, z, t) da. \quad (16)$$

Consider the boundary condition (6) and the velocity field (11) on the surface (3), we obtain

$$\xi + \phi^2 \sigma = 0, \quad \omega + \phi^2 \psi = 0, \quad v_3 + \phi^2 \gamma = 0. \quad (17)$$

The incompressibility condition (4)₂ applied to the velocity field (11), can be written as

$$(v_3)_z + 2\xi + (x_1^2 + x_2^2)(\gamma_z + 4\sigma) = 0. \quad (18)$$

For equation (18) to hold at every point in the fluid, the velocity coefficients must satisfy the conditions

$$(v_3)_z + 2\xi = 0, \quad \gamma_z + 4\sigma = 0. \quad (19)$$

Taking into account (17)_{1,3} these separate conditions (19) reduce to

$$(v_3)_z + 2\xi = 0, \quad (\phi^2 v_3)_z = 0. \quad (20)$$

Now, let us consider a flow in a rigid tube, with lateral wall defined by

$$\phi = \phi(z). \quad (21)$$

Conditions (15), (11), (17)₃ and (20)₂ imply that the volume flow rate Q is just a function of time t , given by

$$Q(t) = \frac{\pi}{2} \phi^2(z) v_3(z, t). \quad (22)$$

Instead of satisfying the momentum equation (4)₁ pointwise in the fluid, we impose the following integral conditions

$$\int_{S(z, t)} \left[\nabla \cdot \mathbf{T} - \rho \left(\frac{\partial \boldsymbol{\vartheta}}{\partial t} + \boldsymbol{\vartheta} \cdot \nabla \boldsymbol{\vartheta} \right) \right] da = 0, \quad (23)$$

$$\int_{S(z, t)} \left[\nabla \cdot \mathbf{T} - \rho \left(\frac{\partial \boldsymbol{\vartheta}}{\partial t} + \boldsymbol{\vartheta} \cdot \nabla \boldsymbol{\vartheta} \right) \right] x_{\alpha_1} \dots x_{\alpha_N} da = 0, \quad (24)$$

where $N = 1, 2, 3$. Using the divergence theorem and integration by parts, equations (23) – (24) for nine directors, can be reduced to the four vector equations:

$$\frac{\partial \mathbf{n}}{\partial z} + \mathbf{f} = \mathbf{a}, \quad (25)$$

$$\frac{\partial \mathbf{m}^{\alpha_1 \dots \alpha_N}}{\partial z} + \mathbf{l}^{\alpha_1 \dots \alpha_N} = \mathbf{k}^{\alpha_1 \dots \alpha_N} + \mathbf{b}^{\alpha_1 \dots \alpha_N}, \quad (26)$$

where $\mathbf{n}, \mathbf{k}^{\alpha_1 \dots \alpha_N}, \mathbf{m}^{\alpha_1 \dots \alpha_N}$ are resultant forces defined by

$$\mathbf{n} = \int_S \mathbf{T}_3 da, \quad \mathbf{k}^\alpha = \int_S \mathbf{T}_\alpha da, \quad (27)$$

$$\mathbf{k}^{\alpha\beta} = \int_S \left(\mathbf{T}_\alpha x_\beta + \mathbf{T}_\beta x_\alpha \right) da, \quad (28)$$

$$\mathbf{k}^{\alpha\beta\gamma} = \int_S \left(\mathbf{T}_\alpha x_\beta x_\gamma + \mathbf{T}_\beta x_\alpha x_\gamma + \mathbf{T}_\gamma x_\alpha x_\beta \right) da, \quad (29)$$

$$\mathbf{m}^{\alpha_1 \dots \alpha_N} = \int_S \mathbf{T}_3 x_{\alpha_1} \dots x_{\alpha_N} da. \quad (30)$$

The quantities \mathbf{a} and $\mathbf{b}^{\alpha_1 \dots \alpha_N}$ are inertia terms defined by

$$\mathbf{a} = \int_S \rho \left(\frac{\partial \boldsymbol{\vartheta}}{\partial t} + \boldsymbol{\vartheta} \cdot \nabla \boldsymbol{\vartheta} \right) da, \quad (31)$$

$$\mathbf{b}^{\alpha_1 \dots \alpha_N} = \int_S \rho \left(\frac{\partial \boldsymbol{\vartheta}}{\partial t} + \boldsymbol{\vartheta} \cdot \nabla \boldsymbol{\vartheta} \right) x_{\alpha_1} \dots x_{\alpha_N} da, \quad (32)$$

and \mathbf{f} , $\mathbf{l}^{\alpha_1 \dots \alpha_N}$, which arise due to surface traction on the lateral boundary, are defined by

$$\mathbf{f} = \int_{\partial S} \sqrt{1 + \phi_z^2} \mathbf{T}_w ds, \quad (33)$$

$$\mathbf{l}^{\alpha_1 \dots \alpha_N} = \int_{\partial S} \sqrt{1 + \phi_z^2} \mathbf{T}_w x_{\alpha_1} \dots x_{\alpha_N} ds. \quad (34)$$

3 Flow in a Tube with Constant Radius

Let us consider a flow in a rigid tube with constant radius, i.e. $\phi = \phi_0 = cts$. Now, taking into account the velocity (11), the stress vector (14), the volume flow rate (22), the average pressure (16), the incompressibility condition (4)₂, the boundary condition (6) and the results quantities (27) – (34) on equations (25) – (26), we obtain

$$\begin{aligned} \bar{p}_z &= - \left(\frac{8\mu}{\pi\phi_0^4} \right) Q(t) - \left(\frac{4\rho\phi_0^2 + 24\alpha_1}{3\pi\phi_0^4} \right) Q_t(t) \\ &+ \omega_z \left(2\alpha_1 + \frac{2}{3}\alpha_2 + \frac{1}{20}\phi_0^2\rho \right) - \omega_{zzz} \frac{\phi_0^2}{30} (\alpha_2 + 2\alpha_1) \\ &+ \omega_z \omega_{zz} \frac{\phi_0^2}{20} (\alpha_2 + 4\alpha_1) \end{aligned} \quad (35)$$

and the wall shear stress

$$\begin{aligned} \tau_1 &= \frac{4\mu}{\pi\phi_0^3} Q(t) + \frac{\rho}{6\pi\phi_0} \left(1 + 24 \frac{\alpha_1}{\rho\phi_0^2} \right) Q_t(t) + \frac{\omega_z \phi_0^3 \rho}{40} \\ &+ (2\alpha_1 + \alpha_2) \left[\frac{\omega_{zzz} \phi_0^3}{60} - \frac{\omega_z \phi_0}{6} + \frac{\omega_z \omega_{zz} \phi_0^3}{30} \right] \end{aligned} \quad (36)$$

where the swirling scalar function $\omega(z, t)$ satisfies the following partial differential equation

$$\begin{aligned} 0 &= 16\omega + \omega_z Q(t) \left(\frac{16\alpha_1}{\pi\mu\phi_0^2} + \frac{6\rho}{5\pi\mu} \right) - \omega_{zz} \phi_0^2 \\ &- \omega_{zzz} Q(t) \frac{6\alpha_1}{5\pi\mu} + \omega_t \left(\frac{16\alpha_1}{\mu} + \frac{\phi_0^2 \rho}{\mu} \right) - \omega_{tzz} \frac{\alpha_1 \phi_0^2}{\mu}. \end{aligned} \quad (37)$$

Considering the viscoelastic coefficients $\alpha_1 = \alpha_2 = 0$ on equation (35) – (37), we recover the swirling Navier-Stokes solution obtained and validated by the work of Caulk and Naghdi, see [6].

Now, let us consider just the steady case. Using the following dimensionless variables³

$$\hat{z} = \frac{z}{\phi_0}, \quad \hat{Q} = \frac{2\rho}{\pi\phi_0\mu} Q, \quad \hat{w} = fw, \quad \hat{\alpha}_1 = \frac{\alpha_1}{\phi_0^2\rho}, \quad \hat{\alpha}_2 = \frac{\alpha_2}{\phi_0^2\rho} \quad (38)$$

on equation (35) – (37), where ϕ_0 is the characteristic radius and f is the Coriolis frequency, we obtain

$$\begin{aligned} \hat{p}_z &= -4\hat{Q} + \mathcal{R}_0 \left[\hat{w}\hat{w}_z \left(2\hat{\alpha}_1 + \frac{2}{3}\hat{\alpha}_2 + \frac{1}{20} \right) \right. \\ &\left. - \hat{w}\hat{w}_{zzz} \left(\frac{\hat{\alpha}_2}{30} + \frac{\hat{\alpha}_1}{15} \right) + \hat{w}_z \hat{w}_{zz} \left(\frac{\hat{\alpha}_2}{20} + \frac{\hat{\alpha}_1}{5} \right) \right] \end{aligned} \quad (39)$$

and the wall shear stress

$$\begin{aligned} \hat{\tau}_1 &= 2\hat{Q} + \mathcal{R}_0 \left[\frac{\hat{w}\hat{w}_z}{40} + (2\hat{\alpha}_1 + \hat{\alpha}_2) \left(\frac{\hat{w}\hat{w}_{zzz}}{60} \right. \right. \\ &\left. \left. - \frac{\hat{w}\hat{w}_z}{6} + \frac{\hat{w}_z \hat{w}_{zz}}{30} \right) \right] \end{aligned} \quad (40)$$

where

$$\mathcal{R}_0 = \frac{\rho^2 \phi_0^4}{f^2 \mu^2}$$

is the Rossby number: a small Rossby number signifies a system which is strongly affected by Coriolis forces, and a large Rossby number signifies a system in which inertial and centrifugal forces dominate. Also, the scalar function $\hat{\omega}(\hat{z})$ satisfies the following ODE

$$0 = 16\hat{\omega} + \hat{\omega}_z \hat{Q} \left(8\hat{\alpha}_1 + \frac{3}{5} \right) - \hat{\omega}_{zz} - \hat{\omega}_{zzz} \hat{Q} \frac{3\hat{\alpha}_1}{5}. \quad (41)$$

Now, integrating condition (39) over a finite section of the tube $[\hat{z}_1, \hat{z}]$, with \hat{z}_1 fixed, we obtain the nondimensional average pressure gradient

$$\begin{aligned} \hat{p}\hat{p}(\hat{z}) &= \hat{p}(\hat{z}_1) - \hat{p}(\hat{z}) \\ &= 4\hat{Q}(\hat{z} - \hat{z}_1) + \mathcal{R}_0 \left[\left(\frac{\hat{\alpha}_2}{30} + \frac{\hat{\alpha}_1}{15} \right) \int_{\hat{z}_1}^{\hat{z}} \hat{w}\hat{w}_{zzz} d\hat{z} \right. \\ &- \left(2\hat{\alpha}_1 + \frac{2}{3}\hat{\alpha}_2 + \frac{1}{20} \right) \int_{\hat{z}_1}^{\hat{z}} \hat{w}\hat{w}_z d\hat{z} \\ &\left. - \left(\frac{\hat{\alpha}_2}{20} + \frac{\hat{\alpha}_1}{5} \right) \int_{\hat{z}_1}^{\hat{z}} \hat{w}_z \hat{w}_{zz} d\hat{z} \right]. \end{aligned} \quad (42)$$

Finally, we observe that the behavior of the average pressure gradient, wall shear stress and swirling effects given by equations (42), (40) and (41) can be numerically illustrated for different values of \mathcal{R}_0 , \hat{Q} , $\hat{\alpha}_1$ and $\hat{\alpha}_2$. In the sequel, when we consider steady flow, the volume flow rate \hat{Q} is identical to the Reynolds number (see [16]). In our applications we consider low Reynolds number, i.e. we have the creeping flow problem.

³In cases where the steady flow rate is specified, the nondimensional flow rate \hat{Q} is identical to the classical Reynolds number used for flow in tubes, see [16].

Taking into account equation (41) and numerical package from *Maple V*, we can show that the steady solution $\hat{\omega}(\hat{z})$, with appropriate initial conditions and $\hat{Q} = 10$, $\hat{\alpha}_1 = -1$, can be approximated by the following Taylor series expansion of order 7

$$\begin{aligned} \hat{\omega}(\hat{z}) = & \hat{z} + \frac{1}{2}\hat{z}^2 + \frac{25}{12}\hat{z}^3 + \frac{47}{96}\hat{z}^4 + \frac{3683}{2880}\hat{z}^5 \\ & + \frac{19751}{103680}\hat{z}^6 + \frac{1627931}{4354560}\hat{z}^7. \end{aligned} \quad (43)$$

Now, we present numerical simulations without physical meaning to the nondimensional average pressure gradient (42) and wall shear stress (40) related with different values of the Rossby number where $\hat{\alpha}_1 = -1$, $\hat{\alpha}_2 = 1$ and $\hat{Q} = 10$ are fixed (see Fig.2 and Fig.3). Shown in Fig.2

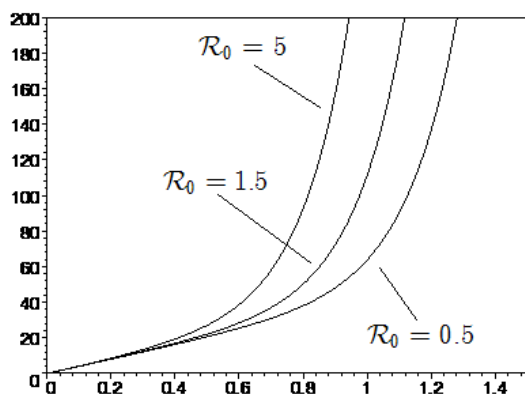


Figure 2: Nondimensional average pressure gradient (42) related with different values of the Rossby number where $\hat{\alpha}_1 = -1$, $\hat{\alpha}_2 = 1$ and $\hat{Q} = 10$ are fixed, and the swirling scalar function $\hat{\omega}(\hat{z})$ is given by (43).

is the nondimensional average pressure gradient (42) for different values of the Rossby number. In this figure, we observe the behavior of the average pressure gradient when we increase the values of the Rossby number with fixed $\hat{\alpha}_1$, $\hat{\alpha}_2$ and \hat{Q} . The exponential behavior of the solution (42) is related with the approximation (43), and also related with the fact that we have a straight tube with constant radius. In this specific geometry the wall shear stress (40) have an interesting behavior induced by the swirling scalar function (43). From Fig.3, we can observe the behavior of the wall shear stress (40) when we increase the values of the Rossby number with fixed $\hat{\alpha}_1$, $\hat{\alpha}_2$ and \hat{Q} .

Several numerical tests have been performed for other values of $\hat{\alpha}_1$, $\hat{\alpha}_2$, \hat{Q} and Rossby numbers, related with the respective swirling scalar function $\hat{\omega}(\hat{z})$, showing similar qualitative results of the average pressure gradient and wall shear stress solutions.

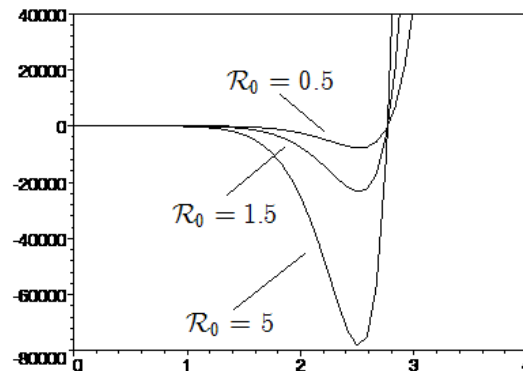


Figure 3: Nondimensional wall shear stress (40) related with different values of the Rossby number where $\hat{\alpha}_1 = -1$, $\hat{\alpha}_2 = 1$ and $\hat{Q} = 10$ are fixed, and the swirling scalar function $\hat{\omega}(\hat{z})$ is given by (43).

4 Flow in a Tube with no Constant Radius

Let us consider a flow in a rigid tube with no constant radius, i.e. $\phi = \phi(z)$. Now, taking into account the dimensionless variables (38) with $\hat{\phi} = \phi/\phi_0$, and using the velocity (11), the stress vector (14), the volume flow rate (22), the average pressure (16), the incompressibility condition (4)₂, the boundary condition (6) and the results quantities (27) – (34) on equations (25) – (26), we obtain the general steady average pressure gradient solution

$$\hat{p}\hat{p}(\hat{z}) = 4\hat{A}(\hat{z})\hat{Q} + \hat{B}(\hat{z})\hat{Q}^2 + \mathcal{R}_0\hat{\Xi}(\hat{z}) \quad (44)$$

where

$$\hat{A}(\hat{z}) = \int_{\hat{z}_1}^{\hat{z}} \frac{\hat{A}}{\hat{\phi}^4} d\hat{z}, \quad \hat{B}(\hat{z}) = \int_{\hat{z}_1}^{\hat{z}} \frac{\hat{B}}{\hat{\phi}^5} d\hat{z}, \quad (45)$$

and

$$\hat{\Xi}(\hat{z}) = \int_{\hat{z}_1}^{\hat{z}} \hat{\Xi} d\hat{z}. \quad (46)$$

The function $\hat{A}(\hat{z})$ is just determined by the geometry of the tube over the interval $I = [\hat{z}_1, \hat{z}]$, with \hat{z}_1 fixed, where

$$\begin{aligned} \hat{A} = & 1 + \frac{1}{3}\hat{\phi}_{\hat{z}}^2 + \frac{1}{16}\hat{\phi}_{\hat{z}}^4 + \frac{1}{3}\hat{\phi}\hat{\phi}_{\hat{z}\hat{z}} + \frac{1}{4}\hat{\phi}\hat{\phi}_{\hat{z}}^2\hat{\phi}_{\hat{z}\hat{z}} \\ & + \frac{1}{32}\hat{\phi}^2\hat{\phi}_{\hat{z}\hat{z}}^2 - \frac{1}{96}\hat{\phi}^3\hat{\phi}_{\hat{z}\hat{z}\hat{z}\hat{z}}. \end{aligned} \quad (47)$$

The function $\hat{B}(\hat{z})$ is determined by the geometry of the tube over the interval I , and also by the viscoelastic coefficients $\hat{\alpha}_1$ and $\hat{\alpha}_2$, where

$$\hat{B} = \hat{B}_1 + \hat{\alpha}_1\hat{B}_2 + \hat{\alpha}_2\hat{B}_3, \quad (48)$$

with

$$\hat{B}_1 = -\hat{\phi}_{\hat{z}} - \frac{3}{40}\hat{\phi}\hat{\phi}_{\hat{z}}\hat{\phi}_{\hat{z}\hat{z}} + \frac{1}{40}\hat{\phi}^2\hat{\phi}_{\hat{z}\hat{z}\hat{z}}, \quad (49)$$

$$\begin{aligned} \hat{B}_2 = & \frac{1}{\hat{\phi}^2} \left(4\hat{\phi}_z + 54\hat{\phi}_z^3 + \frac{19}{2}\hat{\phi}_z^5 - \frac{88}{3}\hat{\phi}_z\hat{\phi}_{zz} \right. \\ & - \frac{49}{6}\hat{\phi}_z^3\hat{\phi}_{zz} + \frac{1}{3}\hat{\phi}_z^2\hat{\phi}_{zz}^2 + 2\hat{\phi}_z^2\hat{\phi}_{zzz} - \frac{1}{6}\hat{\phi}_z^2\hat{\phi}_{zzz}^2 \\ & \left. + \frac{11}{60}\hat{\phi}_z^3\hat{\phi}_{zzz} + \frac{5}{24}\hat{\phi}_z^3\hat{\phi}_{zzz}^2 - \frac{1}{40}\hat{\phi}_z^4\hat{\phi}_{zzz}^2 \right), \end{aligned} \quad (50)$$

and

$$\begin{aligned} \hat{B}_3 = & \frac{1}{\hat{\phi}^2} \left(10\hat{\phi}_z + 30\hat{\phi}_z^3 + \frac{17}{4}\hat{\phi}_z^5 - \frac{44}{3}\hat{\phi}_z\hat{\phi}_{zz} - 3\hat{\phi}_z\hat{\phi}_{zz}^2 \right. \\ & + \frac{2}{3}\hat{\phi}_z^2\hat{\phi}_{zz} - \frac{1}{6}\hat{\phi}_z^2\hat{\phi}_{zz}^2 - \frac{1}{15}\hat{\phi}_z^3\hat{\phi}_{zz} \\ & \left. + \frac{1}{20}\hat{\phi}_z^3\hat{\phi}_{zz}^2 \right). \end{aligned} \quad (51)$$

The function $\hat{\Xi}(\hat{z})$ is determined by the geometry of the tube over the interval I , by the swirling scalar function $\hat{\omega}(\hat{z})$, and also by $\hat{\alpha}_1$ and $\hat{\alpha}_2$, where

$$\begin{aligned} \hat{\Xi} = & \frac{20\hat{\alpha}_2\hat{\omega}^2\hat{\phi}_z}{3\hat{\phi}} + \frac{44\hat{\alpha}_1\hat{\omega}^2\hat{\phi}_z}{3\hat{\phi}} - \frac{2\hat{\alpha}_2\hat{\omega}\hat{\omega}_z}{3} - 2\hat{\alpha}_1\hat{\omega}\hat{\omega}_z \\ & - \frac{3\hat{\omega}^2\hat{\phi}_z}{20} - \frac{\hat{\omega}\hat{\omega}_z\hat{\phi}_z^2}{20} + \frac{\hat{\alpha}_2\hat{\omega}^2\hat{\phi}_z\hat{\phi}_{zz}}{10} + \frac{\hat{\alpha}_1\hat{\omega}^2\hat{\phi}_z\hat{\phi}_{zz}}{5} \\ & - \frac{11\hat{\alpha}_2\hat{\omega}^2\hat{\phi}_z\hat{\phi}_{zz}}{10} - \frac{13\hat{\alpha}_1\hat{\omega}^2\hat{\phi}_z\hat{\phi}_{zz}}{5} + \frac{7\hat{\alpha}_2\hat{\omega}\hat{\omega}_z\hat{\phi}_z\hat{\phi}_{zz}}{30} \\ & + \frac{\hat{\alpha}_1\hat{\omega}\hat{\omega}_z\hat{\phi}_z\hat{\phi}_{zz}}{3} + \frac{4\hat{\alpha}_2\hat{\omega}^2\hat{\phi}_z^3}{5\hat{\phi}} + \frac{4\hat{\alpha}_1\hat{\omega}^2\hat{\phi}_z^3}{5\hat{\phi}} - \frac{\hat{\alpha}_2\hat{\omega}\hat{\omega}_z\hat{\phi}_z^2}{10} \\ & - \frac{19\hat{\alpha}_1\hat{\omega}\hat{\omega}_z\hat{\phi}_z^2}{15} + \frac{7\hat{\alpha}_2\hat{\omega}\hat{\omega}_z\hat{\phi}_z\hat{\phi}_{zz}}{30} + \frac{\hat{\alpha}_1\hat{\omega}\hat{\omega}_z\hat{\phi}_z\hat{\phi}_{zz}}{3} \\ & + \frac{7\hat{\alpha}_2\hat{\omega}_z^2\hat{\phi}_z}{60} - \frac{\hat{\alpha}_1\hat{\omega}_z^2\hat{\phi}_z}{5} - \frac{\hat{\alpha}_1\hat{\omega}_z\hat{\omega}_{zz}\hat{\phi}_z^2}{5} \\ & + \frac{\hat{\alpha}_2\hat{\omega}\hat{\omega}_{zz}\hat{\phi}_z^2}{30} + \frac{\hat{\alpha}_1\hat{\omega}\hat{\omega}_{zz}\hat{\phi}_z^2}{15} - \frac{\hat{\alpha}_2\hat{\omega}_z\hat{\omega}_{zz}\hat{\phi}_z^2}{20}. \end{aligned} \quad (52)$$

In this case, the corresponding wall shear stress is given and by

$$\begin{aligned} \hat{\tau}_1 = & 2\hat{A}'(\hat{z})\hat{Q} + \frac{1}{6}\hat{B}'(\hat{z})\hat{Q}^2 \\ & + \frac{\mathcal{R}_0}{2\hat{\phi}^2(1+\hat{\phi}_z^2)} \left[\frac{\hat{\omega}^2\hat{\phi}_z^4\hat{\phi}_z}{15} + \frac{\hat{\omega}\hat{\omega}_z\hat{\phi}_z^5}{20} \right. \\ & \left. + \hat{\alpha}_1\hat{\Xi}_1 + \hat{\alpha}_2\hat{\Xi}_2 \right], \end{aligned} \quad (53)$$

where the function $\hat{A}'(\hat{z})$ is determined by the geometry of the tube given by

$$\begin{aligned} \hat{A}'(\hat{z}) = & \frac{1}{\hat{\phi}^3(1+\hat{\phi}_z^2)} \left(1 + \frac{1}{3}\hat{\phi}_z^2 + \frac{1}{16}\hat{\phi}_z^4 + \frac{1}{3}\hat{\phi}_z\hat{\phi}_{zz} \right. \\ & + \frac{3}{8}\hat{\phi}_z\hat{\phi}_{zz}^2 + \frac{1}{32}\hat{\phi}_z^2\hat{\phi}_{zz}^2 + \frac{1}{24}\hat{\phi}_z^2\hat{\phi}_z\hat{\phi}_{zzz} \\ & \left. - \frac{1}{96}\hat{\phi}_z^3\hat{\phi}_{zzz}^2 \right), \end{aligned} \quad (54)$$

the function $\hat{B}'(\hat{z})$ is determined by the geometry of the tube, and also by the coefficients $\hat{\alpha}_1$ and $\hat{\alpha}_2$, given by

$$\begin{aligned} \hat{B}'(\hat{z}) = & \frac{1}{\hat{\phi}^4(1+\hat{\phi}_z^2)} \left(-\hat{\phi}_z + \frac{1}{2}\hat{\phi}_z^3 - \frac{19}{40}\hat{\phi}_z\hat{\phi}_{zz} \right. \\ & + \frac{3}{40}\hat{\phi}_z^2\hat{\phi}_{zz} + \frac{\hat{\alpha}_1}{\hat{\phi}^2} \left[74\hat{\phi}_z^3 + 18\hat{\phi}_z^5 - 36\hat{\phi}_z\hat{\phi}_{zz} \right. \\ & - \frac{15}{2}\hat{\phi}_z\hat{\phi}_{zz}^2 - \frac{15}{4}\hat{\phi}_z^2\hat{\phi}_{zz}^2 + 2\hat{\phi}_z^2\hat{\phi}_{zzz} \\ & + \frac{31}{20}\hat{\phi}_z^3\hat{\phi}_{zz} + \frac{7}{8}\hat{\phi}_z^3\hat{\phi}_{zz}^2 \\ & \left. - \frac{3}{40}\hat{\phi}_z^4\hat{\phi}_{zzz} - \frac{7}{2}\hat{\phi}_z^2\hat{\phi}_z\hat{\phi}_{zzz} \right] + \frac{\hat{\alpha}_2}{\hat{\phi}^2} \left[14\hat{\phi}_z^3 \right. \\ & - 6\hat{\phi}_z\hat{\phi}_{zz} + \frac{9}{2}\hat{\phi}_z\hat{\phi}_{zz}^2 - \frac{9}{4}\hat{\phi}_z^2\hat{\phi}_z\hat{\phi}_{zz}^2 \\ & - \frac{3}{2}\hat{\phi}_z^2\hat{\phi}_z\hat{\phi}_{zzz} + \frac{3}{10}\hat{\phi}_z^3\hat{\phi}_z\hat{\phi}_{zzz} \\ & \left. + \frac{3}{20}\hat{\phi}_z^3\hat{\phi}_z\hat{\phi}_{zzz}^2 \right] \Big). \end{aligned} \quad (55)$$

Moreover, the conditions $\hat{\Xi}_1$ and $\hat{\Xi}_2$ are given by

$$\begin{aligned} \hat{\Xi}_1 = & \frac{\hat{\omega}^2\hat{\phi}_z^4\hat{\phi}_z\hat{\phi}_{zz}}{5} - \frac{3\hat{\omega}^2\hat{\phi}_z^3\hat{\phi}_z\hat{\phi}_{zz}}{5} + \hat{\omega}\hat{\omega}_z\hat{\phi}_z^4\hat{\phi}_{zz} \\ & - \frac{6\hat{\omega}^2\hat{\phi}_z^2\hat{\phi}_z^3}{5} - \frac{3\hat{\omega}\hat{\omega}_z\hat{\phi}_z^3\hat{\phi}_z^2}{5} + \frac{2\hat{\omega}\hat{\omega}_{zz}\hat{\phi}_z^4\hat{\phi}_z}{3} \\ & + \frac{4\hat{\omega}_z^2\hat{\phi}_z^4\hat{\phi}_z}{5} + \frac{\hat{\omega}\hat{\omega}_{zzz}\hat{\phi}_z^5}{15} + \frac{2\hat{\omega}_z\hat{\omega}_{zz}\hat{\phi}_z^5}{15} \\ & - \frac{4\hat{\omega}^2\hat{\phi}_z^2\hat{\phi}_z}{3} - 2\hat{\omega}\hat{\omega}_z\hat{\phi}_z^3, \end{aligned} \quad (56)$$

$$\begin{aligned} \hat{\Xi}_2 = & \frac{\hat{\omega}^2\hat{\phi}_z^4\hat{\phi}_z\hat{\phi}_{zz}}{10} - \frac{\hat{\omega}^2\hat{\phi}_z^3\hat{\phi}_z\hat{\phi}_{zz}}{10} + \frac{17\hat{\omega}\hat{\omega}_z\hat{\phi}_z^4\hat{\phi}_z\hat{\phi}_{zz}}{30} \\ & - \frac{6\hat{\omega}^2\hat{\phi}_z^2\hat{\phi}_z^3}{5} - \frac{\hat{\omega}\hat{\omega}_z\hat{\phi}_z^3\hat{\phi}_z^2}{10} + \frac{6\hat{\omega}\hat{\omega}_{zz}\hat{\phi}_z^4\hat{\phi}_z}{15} \\ & + \frac{8\hat{\omega}_z^2\hat{\phi}_z^4\hat{\phi}_z}{15} + \frac{\hat{\omega}\hat{\omega}_{zzz}\hat{\phi}_z^5}{30} + \frac{2\hat{\omega}_z\hat{\omega}_{zz}\hat{\phi}_z^5}{15} \\ & - \frac{4\hat{\omega}^2\hat{\phi}_z^2\hat{\phi}_z}{3} - \frac{2\hat{\omega}\hat{\omega}_z\hat{\phi}_z^3}{3}. \end{aligned} \quad (57)$$

Finally, in this case the swirling scalar function $\omega(z)$ satisfies the following ODE

$$\hat{\omega}\hat{A}_1 + \hat{\omega}_z\hat{A}_2 + \hat{\omega}_{zz}\hat{A}_3 + \hat{\omega}_{zzz}\frac{3\hat{\alpha}_1\hat{\phi}_z^4\hat{Q}}{160} = 0, \quad (58)$$

where

$$\begin{aligned} \hat{A}_1 = & -\frac{3\hat{\phi}^3\hat{\phi}_z\hat{Q}}{80} - \frac{\hat{\alpha}_2\hat{\phi}^3\hat{\phi}_{zzz}\hat{Q}}{40} + \frac{13\hat{\alpha}_2\hat{\phi}^2\hat{\phi}_z\hat{\phi}_{zz}\hat{Q}}{40} \\ & + \frac{\hat{\alpha}_1\hat{\phi}^2\hat{\phi}_z\hat{\phi}_{zz}\hat{Q}}{5} - \frac{3\hat{\alpha}_2\hat{\phi}\hat{\phi}_z^3\hat{Q}}{10} - \frac{3\hat{\alpha}_1\hat{\phi}\hat{\phi}_z^3\hat{Q}}{10} \\ & - \frac{\hat{\alpha}_2\hat{\phi}\hat{\phi}_z\hat{Q}}{2} - \frac{\hat{\alpha}_1\hat{\phi}\hat{\phi}_z\hat{Q}}{2} + \frac{\hat{\phi}^5\hat{\phi}_{zz}}{16} \\ & - \frac{3\hat{\phi}^4\hat{\phi}_z^2}{16} - \frac{\hat{\phi}^4}{2}, \end{aligned} \quad (59)$$

$$\begin{aligned} \hat{A}_2 = & -\frac{3\hat{\phi}^4\hat{Q}}{160} + \frac{\hat{\alpha}_2\hat{\phi}^3\hat{\phi}_{zz}\hat{Q}}{80} + \frac{7\hat{\alpha}_1\hat{\phi}^3\hat{\phi}_{zz}\hat{Q}}{80} \\ & + \frac{\hat{\alpha}_2\hat{\phi}^2\hat{\phi}_z^2\hat{Q}}{80} - \frac{\hat{\alpha}_1\hat{\phi}^2\hat{\phi}_z^2\hat{Q}}{80} - \frac{\hat{\alpha}_1\hat{\phi}^2\hat{Q}}{4} + \frac{\hat{\phi}^5\hat{\phi}_z}{8}, \end{aligned} \quad (60)$$

and

$$\hat{A}_3 = \frac{\hat{\alpha}_2\hat{\phi}^3\hat{\phi}_z\hat{Q}}{80} + \frac{\hat{\alpha}_1\hat{\phi}^3\hat{\phi}_z\hat{Q}}{10} + \frac{\hat{\phi}^6}{32}. \quad (61)$$

Considering the special case $\phi = \phi_0 = cts$ (i.e. $\hat{\phi} = 1$) into equation (44) – (61) we recovered the steady results obtain in last section, i.e. section 3.

Now, let us consider an fluid in a rigid constricted tube (see Fig.4), where the surface function is given by

$$\hat{\phi}(\hat{z}) = 1 + \hat{z}^2, \quad \forall \hat{z} \in [\hat{z}_1, \hat{z}]. \quad (62)$$

Here \hat{z}_1 is fixed, and the maximum tube contraction occurs at $\hat{z} = 0$ and is equal to 1. Taking into account the

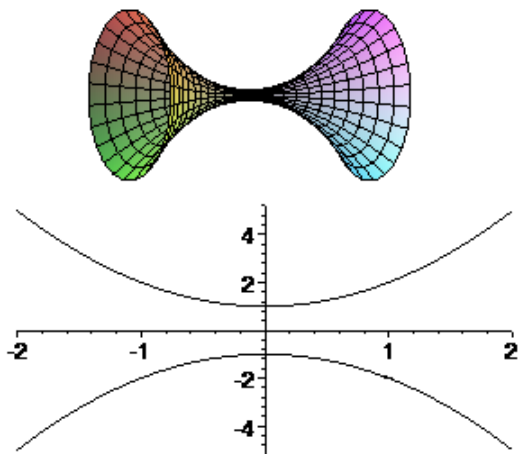


Figure 4: Constricted tube where the surface function is given by condition (62).

surface function (62), equation (58) and numerical package from *Maple V*, we can show that the steady solution $\hat{w}(\hat{z})$, with appropriate initial conditions and $\hat{Q} = 10$,

$\hat{\alpha}_1 = -1, \hat{\alpha}_2 = 1$, can be approximated by the following Taylor series expansion of order 7

$$\begin{aligned} \hat{w}(\hat{z}) = & 2 + \hat{z} + \hat{z}^2 + \frac{1}{9}\hat{z}^3 + \frac{313}{216}\hat{z}^4 + \frac{229}{6480}\hat{z}^5 \\ & - \frac{432767}{233280}\hat{z}^6 - \frac{1330499}{9797760}\hat{z}^7. \end{aligned} \quad (63)$$

Next, we present numerical simulations without physical meaning to the nondimensional average pressure gradient (44) and wall shear stress (53) related with different values of the Rossby number where the viscoelastic coefficients $\hat{\alpha}_1 = -1, \hat{\alpha}_2 = 1$ and the Reynolds number $\hat{Q} = 10$ are fixed (see Fig.5 and Fig.6). Shown in Fig.5

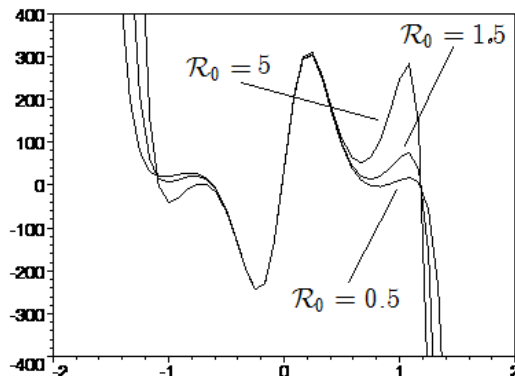


Figure 5: Nondimensional wall shear stress (53) related with different values of the Rossby number where $\hat{\alpha}_1 = -1, \hat{\alpha}_2 = 1$ and $\hat{Q} = 10$ are fixed, and the swirling scalar function $\hat{w}(\hat{z})$ is given by (63).

is the nondimensional wall shear stress (53) for different values of the Rossby number. In this figure, we observe the behavior of the wall shear stress when we increase the value of the Rossby number with fixed $\hat{\alpha}_1, \hat{\alpha}_2$ and \hat{Q} . The behavior of the solution (53) is related with the approximation (63), and also related with the fact that we have a straight tube with no constant radius. In this case, we have undergoes remarkable oscillations for increasing values of the Rossby number. Also, we want to remark the interesting oscillation phenomenon occurs during the contraction of the constricted tube (see interval $[-1, 1]$ in Fig.5). From Fig.6, we can observe the behavior of the average pressure gradient (44) when we increase the values of the Rossby number with fixed $\hat{\alpha}_1, \hat{\alpha}_2$ and \hat{Q} . Here, we remark the constant solution behavior occurs during the contraction of the constricted tube (see interval $[-1, 1]$ in Fig.6).

Several numerical tests have been performed for other values of $\hat{\alpha}_1, \hat{\alpha}_2, \hat{Q}$ and Rossby numbers, related with the respective swirling scalar function $\hat{w}(\hat{z})$, showing similar qualitative results of the average pressure gradient and wall shear stress solutions.

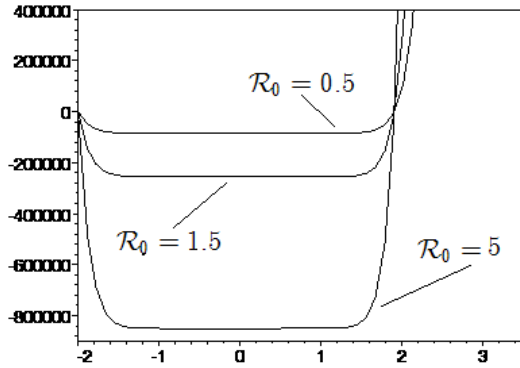


Figure 6: Nondimensional average pressure gradient (44) related with different Rossby numbers where $\hat{\alpha}_1 = -1$, $\hat{\alpha}_2 = 1$ and $\hat{Q} = 10$ are fixed, and the swirling scalar function $\hat{\omega}(\hat{z})$ is given by (63).

5 Conclusions and Future Work

A nine director theory has been used to derive a 1D model in a circular straight rigid and impermeable tube with constant and no constant radius to predict some of the main properties of the 3D Rivlin-Ericksen fluid model with swirling motion. Unsteady/steady relationship between average pressure gradient (wall shear stress, respectively), volume flow rate and the swirling scalar function over a finite section of the tube with constant/no constant radius has been obtained. In this work, we present numerical simulation related with average pressure gradient and wall shear stress for a specific viscoelastic model and geometry like a tube with constant radius, and a constricted tube. One of the possible extensions of this work is the application of this hierarchical approach theory to study *fluid-structure* interaction problems.

References

- [1] Carapau, F., Sequeira, A., "Unsteady flow of a generalized Oldroyd-B fluid using a director theory approach", *WSEAS Transactions on Fluid Mechanics*, Issue 2, V1, pp.167-174, 2006.
- [2] Carapau, F., Sequeira, A., "Axisymmetric motion of a second order viscous fluid in a circular straight tube under pressure gradients varying exponentially with time", *WIT Transaction on Engineering Science*, Issue 1, V52, pp. 409-419, 2006.
- [3] Carapau, F., Sequeira, A., Janela, J., "1D simulations of second-grade fluids with shear-dependent viscosity", *WSEAS Transactions on Mathematics*, Issue 1, V6, pp.151-158, 2007.
- [4] Carapau, F., Sequeira, A., "1D Models for blood flow in small vessels using the Cosserat theory", *WSEAS Transactions on Mathematics*, Issue 1, V5, pp.54-62, 2006.
- [5] Carapau, F., "Average Pressure Gradient of Swirling Flow Motion of a Viscoelastic Fluid in a Circular Straight Tube with Constant Radius", *Proceedings of the International Conference on Mechanical Engineering*, WCE-2009, Imperial College London, London, U.K., 1-3 July, pp.1431-1435, 2009.
- [6] Caulk, D.A., Naghdi, P.M., "Axisymmetric motion of a viscous fluid inside a slender surface of revolution", *Journal of Applied Mechanics*, V54, pp.190-196, 1987.
- [7] Cosserat, E., Cosserat, F., "Sur la théorie des corps minces", *Compt. Rend.*, V146, pp.169-172, 1908.
- [8] Coscia, V., Galdi, G.P., "Existence, uniqueness and stability of regular steady motions of a second-grade fluid", *Int. J. Non-Linear Mechanics*, V29, N4, pp.493-506, 1994.
- [9] Duhem, P., "Le potentiel thermodynamique et la pression hydrostatique", *Ann. École Norm*, V10, pp.187-230, 1893.
- [10] Dunn, J.E., Fosdick, R.L., "Thermodynamics, stability and boundedness of fluids of complexity 2 and fluids of second grade", *Arch. Rational Mech. Anal.*, V56, pp.191-252, 1974.
- [11] Fosdick, R.L., Rajagopal, K.R., "Anomalous features in the model of second order fluids", *Arch. Rational Mech. Anal.*, V70, pp.145-152, 1979.
- [12] Galdi, G.P., Sequeira, A., "Further existence results for classical solutions of the equations of a second-grade fluid", *Arch. Rational Mech. Anal.*, V128, pp.297-312, 1994.
- [13] Green, A.E., Naghdi, P.M., "A direct theory of viscous fluid flow in pipes I: Basic general developments", *Phil. Trans. R. Soc. Lond. A*, Vol.342, pp.525-542, 1993.
- [14] Green, A.E., Naghdi, P.M., Stallard, M.J., "A direct theory of viscous fluid flow in pipes II: Flow of incompressible viscous fluids in curves pipes", *Phil. Trans. R. Soc. Lond. A*, Vol.342, pp.543-572, 1993.
- [15] Rivlin, R.S., Ericksen, J.L., "Stress-deformation relations for isotropic materials", *J. Rational Mech. Anal.*, V4, pp.323-425, 1955.
- [16] Robertson, A.M., Sequeira, A., "A director theory approach for modeling blood flow in the arterial system: An alternative to classical 1D models", *Mathematical Models & Methods in Applied Sciences*, V15, N6, pp.871-906, 2005.